Parametric Study of a Large Active Area PEM Fuel Cell using a MatLab-Simulink Model

S. K. Das* and H. Zhang

Department of Mechanical Engineering
Kettering University
1700 W University Ave, Flint, MI 48504, USA.
*Corresponding author
* Phone: +1-810-762-9916,

Abstract. A Matlab-Simulink based mathematical model and simulation method is developed by applying appropriate physics and electro-chemistry that adequately describes a proton exchange membrane fuel cell (PEMFC) system. The mathematical model is then simulated for a single low temperature PEMFC with a large, 350cm^2, active area. The single cell's performance was evaluated using different operating conditions and varying values of various crucial system parameters. The Matlab-Simulink model presented in this investigation is used to study various parameters' effect such as the cell temperature from 50℃ to 90℃, inlet pressure, relative humidity (RH) from 70% to 90%, and the reactant stoichiometry ratio, on the cell performance. Comparison of polarization and power density curves were conducted between the model simulation and experimental data at 60℃ and at 65℃. Except for the higher current densities range (≥1.6 A/cm^2), the simulation results match with the experimental results very well. The parametric study was used to determine the optimum value of various parameters. The fuel cell performance with the optimized parameter values show a good improvement using the developed MatLab-Simulink model.

Key words. PEMFC, modeling, Matlab-Simulink, fuel cell, experimental validation.

1. Introduction

Over a century, people have been burning fossil fuels as the single main source of energy [1]. The energy demand has increased dramatically year by year, especially in the last few decades [2]. It has become a more and more challenging problem because the combustion of fossil fuels releases greenhouse gasses which have a warming effect in the earth's atmosphere and hence causing extreme weathers globaly. Fossil fuel combustión is also exhausted small particles (i.e., particulate matters) that harm people's health severely [3]. Another problem is the total power production efficiency is very low due to multiple conversions to produce mechanical or electrical energy. Also, fossil fuel is a non-renewable resource and will be used up eventually in the future. A fuel cell is an energy conversion device that converts the chemical energy stored in reactant chemicals directly into electricity. Fuel cells are scalable to form into a stack to get required power output and are highly efficient, producing zero emission and sustainable technology that will help to solve the problems of fossil fuel combustion [1-3]. Among all the fuel cell types, a low temperature PEMFC is under most in-depth investigation in numerous universities, research institutions, and commercial entities. It also is considered to be a widely applied fuel cell system in transportation and various power industries. A fuel cell directly converts chemical energy of the fuel into electrical energy. The laws of thermodynamics are obeyed during the energy conversion process. For a PEMFC, the fuel is hydrogen. A schematic diagram of a PEMFC configuration and basic operating principles are shown in Fig1 [1].
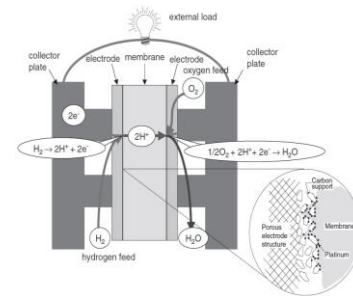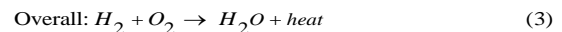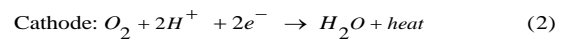

Fig. 1: Basic principle of operation of a PEMFC [1].

The electrochemical reactions in a PEMFC happen simultaneously on both the anode and the cathode as follows [1-2]:

$$\text{Anode: } H_2 \rightarrow 2H^+ + 2e^- \qquad (1)$$

$$\text{Cathode: } O_2 + 2H^+ + 2e^- \rightarrow H_2O + heat \qquad (2)$$

$$\text{Overall: } H_2 + O_2 \rightarrow H_2O + heat \qquad (3)$$

The basic construction of a PEMFC is shown in Fig. 2. It contains the FP-flow plates, GDL-gas diffusion layers, CL-catalyst layer, and PEM-polymer electrolyte membrane. The combination of FP + GDL + CL is also known as anode which is for H_2 or cathode for air or O_2 [1-3].
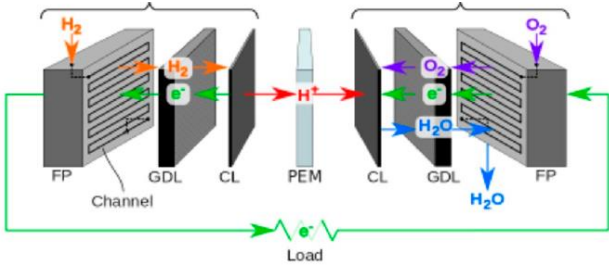

Fig. 2: Basic construction of a PEMFC [1-3].

Predicting the performance of a PEMFC is very critical for the required power system design, however, it is well known that fabrication and testing of PEMFC prototypes are expensive in both time and cost. Modeling and simulation are the easiest and convenient process of applying appropriate fundamental laws to derive mathematical equations that adequately describe the physics and electro-chemistry of the PEMFC system, and then predict the system performance and eventually develop a actual prototype based on the simulation results for experimental evaluation. For the sake of geometry selection of the mathematical model, it can be classified as 1-dimensional (1D), 2-dimensional (2D) and 3-dimensional (3D) models. Since in a fuel cell, the only byproducts are wáter and heat, hence to optimize the efficiency and lifecycle of a fuel cell; the reactant gas supply, water management and heat management subsystems need to be controlled properly during both steady-state and transient operations. Many researchers have started modeling and simulation Works of fuel cell systems from 1D to 3D using various softwares or user defined codes.

Pukrushpan et al. [4] employed modeling and multivariable control techniques to provide fast and consistent system dynamic behavior. They created a framework by Matlab-Simulink tools for analyzing and evaluating different control architectures and sensor sets. Xiao et al. [5] created dynamic and thermodynamic models based on the Matlab-Simulink environment. These models are then implemented through the graphic user interface (GUI) programming by Simulink, and the simulation results are visualized. They analyzed the voltage overshoots and undershoots in the simulation results, which came from the combination of a electrical dynamic model and a thermodynamic model. Jia et al. [6] developed a dynamic model of a PEM fuel cell with Matlab-Simulink to investigate the output characteristics of a PEM fuel cell. By using a fuel cell test system, they conducted and analyzed the transient electrical response of the PEM fuel cell system under various operating conditions.

Abdin et al. [7] described and realized a PEM fuel cell mathematical model in four ancillaries in the Matlab-Simulink environment and empirically described the characteristics of the fuel cell. Chavan et al. [8] proposed a simple but more realistic Matlab-Simulink model for a PEM fuel cell to evaluate its performance under different conditions with $25cm^2$ active área. Recently, Das and Gibson [3] simulated a 3D model of high temperatura PEMFC and assessed the effect of mass transport limitations on the performance of the fuel cell. In this study, we developed a complete low temperatura PEMFC with a large active área of $350cm^2$ by including all subdomains together as shown in Fig. 2 using Matlab-Simulink software package. The simulation model is validated with experimental results and conducted a parametric studies to optimized various parameters. The optimized parameter values was used the study the cell performance.

2. Model Governing Equations and Simulation Method

To analyze the performance of a PEMFC, the understanding of the internal reactions and various processes that take place inside it is very crucial. Physical phenomena occurring within a PEM fuel cell can be represented by the conservation equations for mass, momentum, energy, species, and current transport. To reduce the complexity of the simulation model, the following assumptions were used in the Matlab-SImulink model for the low temperature PEMFC: (i) The PEMFC operates at steady-state. (ii) The operating temperature is homogeneous in all the reactants, products and areas of the PEMFC. (iii) Only water vapor exists in the reactant flows and the relative humidity (RH) is homogeneous in all the reactants, products and areas of the PEMFC. (iv) All the gas species are considered as ideal gas or ideal gas mixtures. (v) All the reactant gasses follow laminar flow since the operating pressure and velocity are low enough. (vi) All the porous media (GDL, CL and membrane) are considered to be continuous, isotropic and non-deformable structures. (vii) The reactants react completely in the catalyst layer. (viii) The produced water is drained completely in time and produced heat is managed appropriately.

At any point (location) in the gas diffuser and the gas channel, the total mass and momentum conservation can be written as [1, 3]:

$$\varepsilon \frac{\partial \rho}{\partial t} + \nabla \cdot (\varepsilon \rho \mathbf{u}) = 0, \qquad (4)$$

$$\frac{\partial (\varepsilon \rho \mathbf{u})}{\partial t} + \nabla \cdot (\varepsilon \rho \mathbf{u}\mathbf{u}) = -\varepsilon \nabla p + \nabla \cdot (\varepsilon \mu \nabla \mathbf{u}), \qquad (5)$$

where ε is the porosity and it equals 1 in the flow channels, $\mathbf{u}$ is the velocity vector, t is the time, p stands for pressure, μ denotes dynamic viscosity and ρ is the density can be found using ideal gas law defined as [3]:

$$\rho = \frac{PM}{RT}. \qquad (6)$$

where M represents the molar mass of reactant gases, T is the temperature and R denotes ideal gas constant. Darcy's law is usually used to describe the flow within the porous media and can be written as [3]:

$$\nabla p = -\frac{\mu}{k_p}(\varepsilon \mathbf{u}), \tag{7}$$

where k_p stands for absolute permeability. The general species conservation equation for the multi-species mixture in gas diffuser describe by Maxwell-Stefan type equation [3,9] as:

$$\varepsilon \frac{\partial}{\partial t}(\rho C^\alpha) + \nabla \cdot (\rho \mathbf{u} C^\alpha) = \nabla \cdot \left(\varepsilon \rho \sum_j D_j^\alpha \nabla C^\alpha \right) + S_\alpha, \tag{8}$$

where C represents concentration of species, D is the diffusion constant, and α and j denote different species which includes hydrogen, oxygen, nitrogen and water vapor. S_α is the source term represents the reaction rate accounted for the consumption of reactant gases and formation of chemical products through electro-chemical reactions at the electrodes. The source term S_α was considered as follows:

$$\left. \begin{aligned} S_{H_2} &= -\frac{j_a}{2F} M_{H_2} \\ S_{O_2} &= \frac{j_c}{4F} M_{O_2} \\ S_{H_2O} &= -\frac{j_c}{2F} M_{H_2O} \end{aligned} \right\} \tag{9}$$

where Mi represents the molar mass of specific species, F is the Faraday constant, ja and jc are the exchange/transfer current density at anode and cathode respectively. The binary diffusion coefficients in equation (5) can be calculated using the following relationship [3,9].

$$D_j^\alpha = D_j^0 \left(\frac{T}{T_0} \right)^{1.5} \tag{10}$$

where D_j^0 is the reference diffusion coefficient, T_0 is the reference temperature and T is the cell temperature. The Bruggeman's correlation, related to the tortuosity and porosity of porous media, was used to correct the binary diffusion coefficient and determined the effective binary diffusion coefficients on GDL layers as [3,9]

$$D_j^\alpha \big|_{effective} = (\varepsilon)^{1.5} D_j^\alpha \tag{11}$$

The charge balance equation in the porous electrodes and in the membrane can be written by using Ohm's law as [3]:

$$\left. \begin{aligned} -\nabla \cdot \left(\sigma_s^{eff} \nabla \Phi_s \right) + S_s &= 0 \\ \nabla \cdot \left(\sigma_m^{eff} \nabla \Phi_m \right) + S_m &= 0 \end{aligned} \right\} \tag{12}$$

where Φ is the potential, subscript s denotes the solid media for the electron potential and m represents the membrane or electrolyte media for the ionic potential due to proton transfer, σ denotes the conductivity in the respective media, S_s and S_m represent the source terms arise from the electro-chemical reactions occurred at the anode and cathode catalyst layers, and proton transport through the membrane which can be defined as [3]:

$$\left. \begin{aligned} &\text{at anode catalyst layer: } S_s = -j_a, \ S_m = j_a \\ &\text{at cathode catalyst layer: } S_s = -j_c, \ S_m = j_c \end{aligned} \right\} \tag{13}$$

where the transfer current density related to the electro-chemical reaction at anode, j_a, and at cathode, j_c, can be represented by the Butler-Volmer equations defined as [3]:

$$j_a = A j_{0,a}^{ref} \left(\frac{C^{H_2}}{C_{ref}^{H_2}} \right)^{1/2} \left[\exp\left(\frac{\alpha_a F \eta}{RT} \right) - \exp\left(-\frac{\alpha_c F \eta}{RT} \right) \right] \tag{14}$$

$$j_c = A j_{0,c}^{ref} \left(\frac{C^{O_2}}{C_{ref}^{O_2}} \right)^{1/2} \left[\exp\left(\frac{\alpha_a F \eta}{RT} \right) - \exp\left(-\frac{\alpha_c F \eta}{RT} \right) \right] \tag{15}$$

where A is the catalyst surface area per unit volume, $j_{0,a}^{ref}$ and $j_{0,c}^{ref}$ are reference exchange current densities at anode and cathode respectively, α_a and α_c are the charge transfer coefficient at anode and cathode respectively, and η is the surface over-potential defined as:

$$\eta = \Phi_s - \Phi_m - V_{oc} \tag{16}$$

where Φ_s and Φ_m stand for the potentials of the electronically conductive solid and potentials through the membrane or electrolyte, respectively. V_{oc} is the reference open-circuit potential of an electrode. It is equal to zero on the anode but is a function of temperature on the cathode [3], namely:

$$V_{0c,+} = 0.0025T + 0.2329 \tag{17}$$

where T is in Kelvin and V_{oc} is in volts.

The energy conservation equations for the multi-species transport can be written as [3]:

$$\nabla \cdot \left(\rho c_p \mathbf{u} T \right) = \nabla \cdot \left(k^{eff} \nabla T \right) + S_T, \tag{18}$$

where T is the temperature, c_p is the specific heat at constant pressure and k^{eff} is the effective thermal conductivity of the materials. The thermal source term, S_T can be written as [3]:

$$\left. \begin{aligned} &\text{at anode: } S_T = j_a \eta + \frac{I^2}{k^{eff}} \\ &\text{at cathode: } S_T = j_c \eta + \frac{I^2}{k^{eff}} + j_c \frac{dV_{oc}}{dT} T \end{aligned} \right\} \tag{19}$$

In order to solve the model equations (4)-(19), appropriate boundary and initial conditions are required at various boundaries, interfaces, inlets and outlets for the multi-species mixture model of the LT-PEMFC presented in Fig. 2. The fuel and oxidant flow rate at the anode and cathode flow channel can be described by a

stoichiometric flow ratio, ξ, defined as the amount of reactant in the flow channel gas feed divided by the amount required by the electrochemical reaction at the electrode. That is

$$\xi_{cathode} = C_0^{O_2}\vartheta^0 + \frac{P_{cathode}}{RT_{cathode}}\frac{4F}{I_{ref,c}A_c} \tag{20}$$

$$\xi_{anode} = C_0^{H_2}\vartheta^0 - \frac{P_{anode}}{RT_{anode}}\frac{2F}{I_{ref,a}A_a} \tag{21}$$

where ϑ^0 is the inlet volumetric flow rate to a gas channel, P and T are the pressure and temperature respectively, R and F are the universal gas constant and Faraday's constant respectively, I is the current density, and A is the electrode surface area. For convenience, the stoichiometric flow ratios defined in equations (20) and (21) are based on the reference current density of I_{ref} (A/cm^2) here so that the ratios can also be considered as dimensionless flow rates of the fuel and oxidant. For velocity and pressure (i.e. for $\mathbf{u}$ and p), the Navier-Stokes equations in the flow channels were solved using the conditions:

$$\left. \begin{array}{l} \text{at anode: } u_{inlet} = \frac{\xi_{anode}A_{mem}}{C^{H_2}A_{channel}}, \ p_{channel\ outlet} = p_{atm} \\[2ex] \text{at cathode: } u_{inlet} = \frac{\xi_{cathode}A_{mem}}{C^{O_2}A_{channel}}, \ p_{channel\ outlet} = p_{atm} \end{array} \right\} \tag{22}$$

For charge balance:

$$\left. \begin{array}{l} \text{at anode: } \Phi_s = 0 \\[1ex] \text{at cathode: } \Phi_s = V_{cell} \left(\text{voltage condition i.e. } \Phi_s = -dV \right) \end{array} \right\} \tag{23}$$

For outlet/Interior boundaries: Fully developed steady-state laminar flow, channel symmetry and no-flux (i.e. insulation) conditions are applied.

$$\frac{\partial C_k^\alpha}{\partial n} = 0, \ \frac{\partial p}{\partial n} = 0, \ \frac{\partial \Phi_e}{\partial n} = 0, \ \frac{\partial \Phi_s}{\partial n} = 0. \tag{24}$$

At the wall boundaries:
No-slip and impermeable velocity condition, and no-flux conditions are applied.

$$\mathbf{u} = 0, \ \frac{\partial \mathbf{u}}{\partial n} = 0, \ \frac{\partial C_k^\alpha}{\partial n} = 0, \ \frac{\partial p}{\partial n} = 0, \ \frac{\partial \Phi_e}{\partial n} = 0, \ \frac{\partial \Phi_s}{\partial n} = 0. \tag{25}$$

The geometry presented in Fig. 2 incorporated all subdomains of a LT-PEMFC in the simulation model. The model governing equations (4)-(19) were numerically solved in stages numerically using Matlab-Simulink based software tool with the boundary and initial conditions given in equations (20)-(25). Various source terms and physio-electro-kinetics properties were incorporated in the simulation model by customizing MatLab-Simulink software's user defined interface module. A schematic of the developed MatLab-Simulink model of a single low temperatura PEMFC is shown in Fig. 3.

3. Results and Discussions

First we validated our developed MatLab-Simulink based model of a single low temperatura PEMFC (LT-PEMFC) model simulation results with the experimental results using the Nafion 111 membrane characteristics. Both

polarization curves and power density curves are shown in Fig. 4 using the model simulation results and experimental results [10]. The cell temperatures of both the experimental and simulation results were obtained at 60°C and 65°C. The relative humidity (RH) was 90%, the stoichiometry of H_2 was 1.2 and the stoichiometry of air was 2.0 [10-11]. The experimental data from the current at 1.6A/cm² to 2.0A/cm² were not available, but the simulation data presented up to 2.0A/cm² to show the complete polarization curves and power density curves.
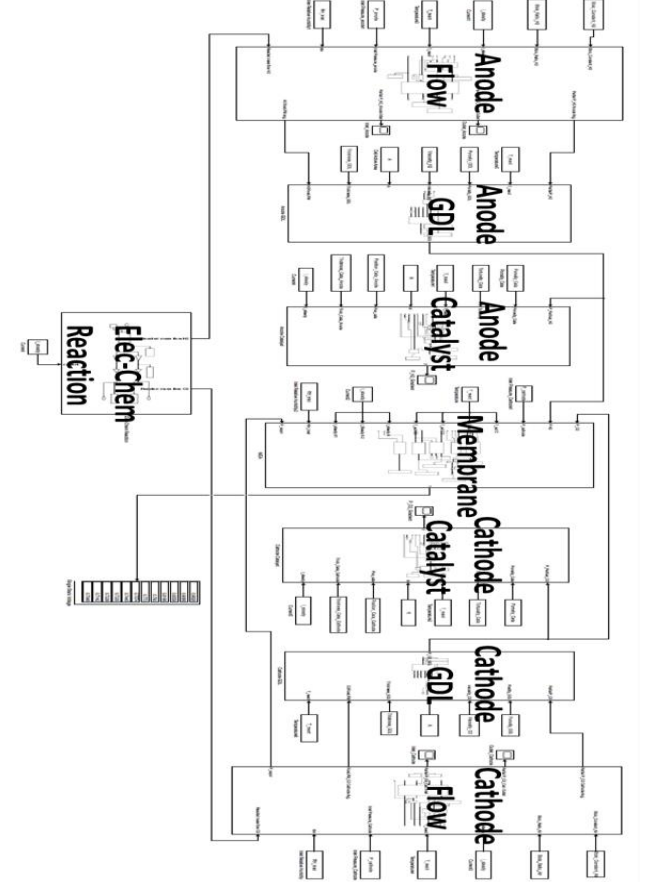

Fig. 3: Schematic of the MatLab-Simulink model of a single LT-PEMFC.

From Fig. 4, we can see that the overall trends of the cell voltage and power densities as a function of current densities from 0 to 1.6 A/cm² match very well between the simulation and experimental results. It indicated that the developed MatLab-Simulink based model can be used to study the parametric impact on the low temperature PEM fuel cell performance.

3.1 Results of Parametric Study

In this section, a parametric study was performed using the developed Matlab-Simulink LT-PEMFC simulation model to understand the impact of each parameter on the LT-PEMFC performance. With all the parameters and variables being kept constant such as the membrane relative humidity is at 90%, the H_2 stoichiometry is 1.2 and the air stoichiometry is 2.0, the simulation model was run at temperatures of 50°C, 60°C, 65°C, 70°C, 75°C, 80°C, 85°C, and 90°C. The current densities were kept at

from 0.00 to 2.00 A/cm², the polarization curves and power density curves obtained from the Matlab-Simulink model are as shown in Fig. 5. From Fig. 5, it can be found that the cell temperature shows significant impact on the cell voltage at various current densities, a higher cell temperature will create higher cell voltage and hence a higher cell power at the same current density.
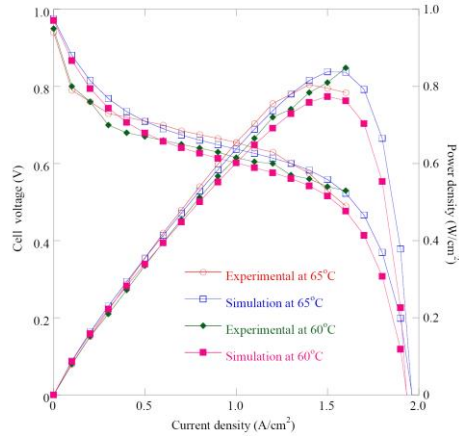

Fig. 4: Comparison of experimental and model simulation results of polarization and power density curves of a single LT-PEMFC.
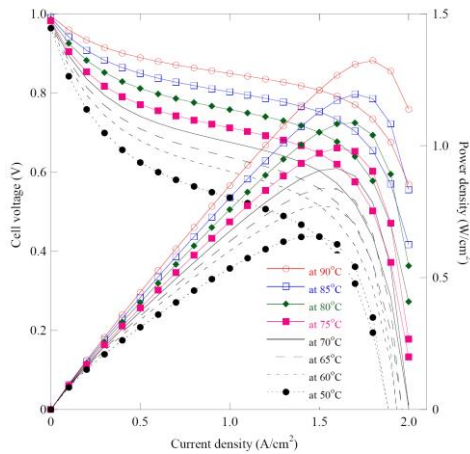

Fig. 5: Polarization and power density curves of a single LT-PEMFC at different cell temperatures.

With all the parameters and variables being kept constant as shown such as the cell temperature is at 75°C, the H_2 stoichiometry is at 1.2 and the air stoichiometry is at 2.0, the simulation model was run at various relative humidity from 70% to 90%. The the polarization curves and power density curves obtained from the Matlab-Simulink model are shown in Fig. 6. From Fig. 6, it is found that the higher membrane relative humidity increases higher cell voltage and cell power at the same current density. The most significant impact of relative humidity on cell voltage occurs at the higher current density range from 0.8 to 1.9A/cm² as can be seen from Fig. 6.

Fig.7 represents the polarization and power density curves of a single LT-PEMFC at different membrane conductivities while all other parameters kept constant such as the cell temperature is at 75°C, the H_2 stoichiometry is at 1.2 and the air stoichiometry is at 2.0, the relative humidity is at 90%, the GDL thickness is 38μm and GDL porosity is 80%. The Matlab-Simulink

Lt-PEMFC model was simulated at membrane conductivities of 10S/cm, 20S/cm, and 30S/cm. It is found from Fig. 7 that the membrane conductivity shows significant impact on the cell voltage at various current densities. A higher membrane conductivity will result in higher cell voltage and power at the same current density. The impact of membrane conductivity on the cell voltage and power is very profound at the higher current density range from 0.6 to 2.0 A/cm² as can be seen in Fig. 7.
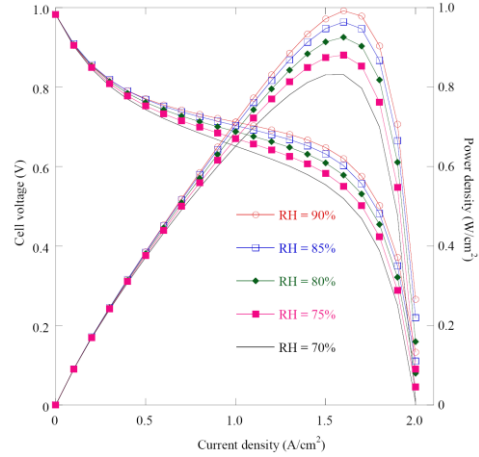

Fig. 6: Polarization and power density curves of a single LT-PEMFC at different membrane relative humidity.
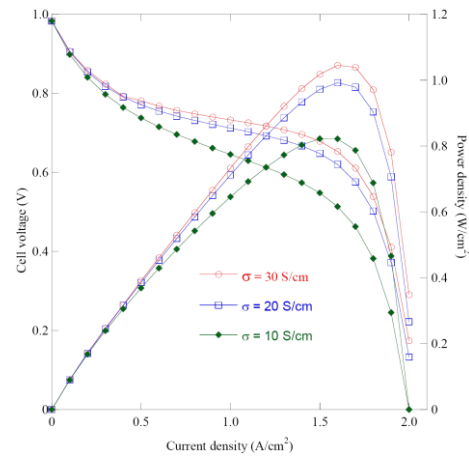

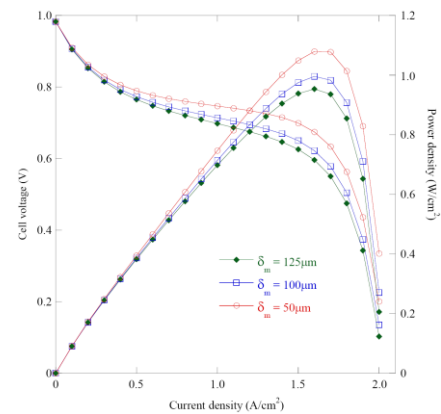Fig. 7: Polarization and power density curves of a single LT-PEMFC at various membrane conductivities, σ.

Fig. 8: Polarization and power density curves of a single LT-PEMFC at various membrane thicknesses, δ_m.

Fig. 8 represents the polarization and power density curves of a single LT-PEMFC at different membrane thickness. From Fig. 8, it can be seen that higher membrane thickness resulted lower cell performance due to higher resistance imposed on the ionic conduction through the thicker membranes.

Analyzing the parametric study results, an optimized value of each parameter was determined. Using the optimized parameters values as shown in Table 1, a model simulation of PEMFC was conducted with the cell temperature at 75°C, the H_2 stoichiometry at 1.2 and the air stoichiometry at 2.0, the relative humidity is at 90%, the GDL thickness is 38μm and GDL porosity is 80%, the membrane conductivity is 20 S/cm, and the membrane thickness is 100μm, the current densities were ranged from 0.0 to 2.0 A/cm^2.

Table 1. Optimized parameter values for a single LT-PEMFC model simulation.

Temperature	75°C	RH	90%
Stoich Anode (H_2)	1.2	Stoich Cathode (air)	2.0
Thickness δ_{GDL}	0.038mm	Porosity ε_{GDL}	80%
Thickness δ_m	0.1mm	Conductivity σ_m	20 S/cm

Comparison of polarization and power density curves of a single LT-PEMFC using the optimized parameter values listed in table 1 with the experimental results at 65°C is shown in Fig. 9. From Fig. 9, it can be seen that both the polarization and power density curves of the LT-PEMFC improved significantly with the optimized parameter values compared to the experimental results. It is noted that the simulation results with optimized parameter values was with cell temperatura of 75°C compared to the experimental results at 65°C. Even though there is a 10°C difference of the cell operating temperature between the simulation and experimental results, it can be seen that the cell performance is quite improved with the optimized parameters values compared to the cell performance impacted by the cell temperature difference as can be seen from Fig. 5 and Fig. 9.
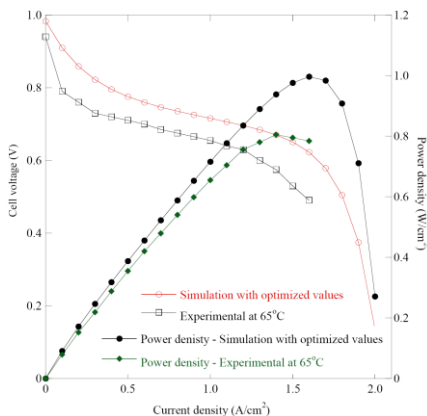

Fig. 9: Comparison of polarization and power density curves of a single LT-PEMFC with optimized parameter values given at Table 1 with the experimental results at 65°C.

4. Conclusion

In this study, a Matlab-Simulink based model of a single LT- PEMFC with a large active área of 350cm^2 is developed and studied to understand various parameters effect on the cell performance. The simulation results of the developed Matlab-Simulink model matches very well with the experimental data at 60°C and at 65°C. The simulation results showed that various important parameters significantly impact the performance of the LT-PEMFC. The simulation results with optimized paramter values showed improved cell performance compared to the experimental results. The results presented in this study with developed Matlab-Simulink model will enhance the overall understanding of the single LT-PEMFC operation and help to design optimized multi-cells stack of the LT-PEMFC system.

References
[1] Barbir, Frano, *PEM Fuel Cells: Theory and Practice*. Elsevier Science & Technology, 2013.
[2] R. O'Hayre, S. W. Cha, W. Colella, F. B. Prinz, *Fuel Cell Fundamentals*. Hoboken, NJ, USA: John Wiley & Sons , 2016.
[3] S. K. Das and H. A. Gibson, " Three dimensional multi-physics modeling and simulation for assessment of mass transport impact on the performance of a high temperature polymer electrolyte membrane fuel cell," *Journal of Power Sources*, vol. 499, p. 229844, 2021.
[4] J. T. Pukrushpan *et al.*, *Control of Fuel Cell Power Design*. London, UK: Springer-Verlag, 2004.
[5] Y. Xiao and K. Agbossou, "Interface design and software development for PEM fuel cell modeling based on Matlab-simulink environment," *IEEE Computer Society*, vol. 4, pp. 318-322, 2009.
[6] J. Jia *et al.*, " Modeling and dynamic characteristic simulation of a proton exchange membrane fuel cell," *IEEE Transactions on Energy Conversion*, vol. 24, no. 1, pp. 283-291, Mar. 2009.
[7] Z. Abdin *et al.*, "PEM fuel cell model and simulation in Matlab-simulink based on physical parameters," *Energy*, vol. 116, pp. 1131-1144, 2016.
[8] S. L. Chavan and D. B. Talange, "Modeling and performance evaluation of PEM fuel cells by controlling its input parameters," *Energy*, vol. 138, pp. 437-445, 2017.
[9] D. Niblett, A. Mularczyk, V. Niasar, J. Eller, S. Holmes, " Two-phase flow dynamics in a gas diffusion layer-gas channel-microporous layer system," *J. Power Sources*, vol. 471, p. 228427, 2020.
[10] E. U. Ubong and K. D. Susanta, " Validating theoretical models with experimental data in two PEM fuel cells categories," in *Proceedings of the Second European Fuel Cell Technology and Applications Conference*, Dec. 2007, ASME, EFC2007-39154.
[11] S. K. Das, A. Reis, and K. J. Berry, " Experimental evaluation of CO poisoning on the performance of a high temperature proton exchange membrane fuel cells," *J. Power Sources*, vol. 193, pp. 691-698, 2009.